1521-009X/43/7/1091–1099$25.00
Drug Metabolism and Disposition
http://dx.doi.org/10.1124/dmd.115.063495
Drug Metab Dispos 43:1091–1099, July 2015

Metabolite Profiling and Pharmacokinetic Evaluation of Hydrocortisone in a Perfused Three-Dimensional Human Liver Bioreactor[S]

Ujjal Sarkar, Dinelia Rivera-Burgos, Emma M. Large, David J. Hughes, Kodihalli C. Ravindra, Rachel L. Dyer, Mohammad R. Ebrahimkhani, John S. Wishnok, Linda G. Griffith, and Steven R. Tannenbaum

Department of Biological Engineering (U.S., D.R.-B., K.C.R., R.L.D., M.R.E., J.S.W., L.G.G., S.R.T.), Department of Chemistry (S.R.T.), and Department of Mechanical Engineering (L.G.G.), Massachusetts Institute of Technology, Cambridge, Massachusetts; and CN Bio Innovations, Oxford University Begbroke Science Park, Begbroke, Oxfordshire, United Kingdom (E.M.L., D.J.H.)

Received January 23, 2015; accepted April 29, 2015

ABSTRACT

Endotoxin lipopolysaccharide (LPS) is known to cause liver injury primarily involving inflammatory cells such as Kupffer cells, but few in vitro culture models are applicable for investigation of inflammatory effects on drug metabolism. We have developed a three-dimensional human microphysiological hepatocyte–Kupffer cell coculture system and evaluated the anti-inflammatory effect of glucocorticoids on liver cultures. LPS was introduced to the cultures to elicit an inflammatory response and was assessed by the release of proinflammatory cytokines, interleukin 6 and tumor necrosis factor α. A sensitive and specific reversed-phase–ultra high-performance liquid chromatography–quadrupole time of flight–mass spectrometry method was used to evaluate hydrocortisone disappearance and metabolism at near physiologic levels. For this, the systems were dosed with 100 nM hydrocortisone and circulated for 2 days; hydrocortisone was depleted to approximately 30 nM, with first-order kinetics. Phase I metabolites, including tetrahydrocortisone and dihydrocortisol, accounted for 8–10% of the loss, and 45–52% consisted of phase II metabolites, including glucuronides of tetrahydrocortisol and tetrahydrocortisone. Pharmacokinetic parameters, i.e., half-life, rate of elimination, clearance, and area under the curve, were 23.03 hours, 0.03 hour^{-1}, 6.6 × 10^{-5} l·hour^{-1}, and 1.03 (mg/l)*h, respectively. The ability of the bioreactor to predict the in vivo clearance of hydrocortisone was characterized, and the obtained intrinsic clearance values correlated with human data. This system offers a physiologically relevant tool for investigating hepatic function in an inflamed liver.

Introduction

Inflammation of the liver may result from infection, autoimmune disorders, alcohol abuse, or fat accumulation (Adams et al., 2010). Severe inflammation can be life-threatening, whereas mild inflammation can change drug metabolism profiles (Adams et al., 2010) and may play a role in liver injury (Park et al., 2004; Deng et al., 2009). Drug-induced liver injury has resulted in late-stage clinical trial failures and postmarket withdrawals (Guengerich, 2011).

A postulated mechanism for toxicity involves leakage of bacterial products from the gut to the liver, causing inflammation-related susceptibility to liver injury (Deng et al., 2008). This has been demonstrated in animal models (Roth et al., 2003; Deng et al., 2009; Roth and Ganey, 2010) but could be supported by a human-derived in vitro model that recapitulates the response of liver to inflammation. The simplest model is the two-dimensional culture of primary hepatocytes, either as a monolayer or overlaid with extracellular matrix components in multiwall plates. Through exogenous addition of cytokines or other inflammatory stimuli to the cultures, two-dimensional hepatocyte monocultures can probe inflammation-associated drug hepatotoxicity (Cosgrove et al., 2009). The absence of macrophages, however, makes it unsuitable for modeling anti-inflammatory effects.

Numerous advanced liver models, which improve the long-term functional performance of hepatocytes compared with monocultures, have been described (Groothuis and Meijer, 1992; LeCluyse et al., 2012); a subset of these incorporates liver nonparenchymal cells in coculture (Maier and Milosevic, 1999; Milosevic et al., 1999; Zinchenko et al., 2006; Dash et al., 2009; Domansky et al., 2010; Kostadinova et al., 2013). For inflammatory models, cultures containing Kupffer cells—either added as a separate fraction or as part of a whole nonparenchymal fraction—are most relevant. In these systems, the nonparenchymal cell fraction or Kupffer cells may be mixed with hepatocytes to form heterogeneous aggregates (Drewitz et al., 2011; Messner et al., 2013;

This research was supported by the United States Defense Advanced Research Projects Agency [grant W911NF-12-2-0039], the National Institutes of Health [grant 5-UH2-TR000496], and the Massachusetts Institute of Technology Center for Environmental Health Sciences [grant P30-ES002109].

U.S. and D.R.-B. contributed equally to this work.

dx.doi.org/10.1124/dmd.115.063495.

[S]This article has supplemental material available at dmd.aspetjournals.org.

ABBREVIATIONS: ACN, acetonitrile; AUC, area under the curve; CAS, chemical abstract service; CL, clearance; CL_h, predicted hepatic clearance; CL_{int}, intrinsic clearance; $CL_{int\text{-}in\ vivo}$, in vivo intrinsic clearance; 3D, three-dimensional; FA, formic acid; HC, hydrocortisone; HSA, human serum albumin; IL6, interleukin 6; IVIVC, in vitro/in vivo correlation; LC, liquid chromatography; LPS, lipopolysaccharide; MS, mass spectrometry; NPC, nonparenchymal cell; QTOF, quadrupole time of flight; RP, reversed-phase; $t_{1/2}$, half-life; MS/MS, tandem mass spectrometry; TNFα, tumor necrosis factor α; UHPLC, ultra-high-performance liquid chromatography; WEM, Williams' E medium.

Thoma et al., 2014), supported on a scaffold (Dash et al., 2009; Kostadinova et al., 2013), or separated through micropatterning (Zinchenko et al., 2006). Transwell devices have also been evaluated (Milosevic et al., 1999). Hoebe et al. (2000, 2001) showed that direct cell-to-cell contact between porcine hepatocytes and Kupffer cells increased the inhibitory effects of lipopolysaccharide (LPS) stimulation on testosterone metabolism. Hepatocyte and Kupffer cell models have also been applied to the study of Kupffer cell suppression of cytochrome P450–mediated metabolism in humans (Sunman et al., 2004) and rat cells (Milosevic et al., 1999). Models based on hepatocytes and a mixed nonparenchymal cell fraction system have also been used to explore exaggerated hepatotoxicity in conjunction with an underlying inflammation (Dash et al., 2009; Drewitz et al., 2011; Messner et al., 2013; Thoma et al., 2014).

Cortisol and, more typically the more potent synthetic glucocorticoid, dexamethasone are used at nanomolar to micromolar concentrations in cultures of primary hepatocytes to maintain a differentiated state (Hewitt et al., 2007; Scheving et al., 2007; Godoy et al., 2010). In a coculture of rat hepatocytes and epithelial cells, cortisol increased albumin secretion and extracellular matrix production (Baffet et al., 1982; Guillouzo et al., 1984).

Cortisol, the major glucocorticoid in humans, is produced in the adrenal cortex, regulated both by diurnal rhythms and in response to stress (Morse and Davis, 1990). When used as a drug, it is referred to as hydrocortisone, and it acts in vivo as an anti-inflammatory and suppresses immune responses (Perogamvros et al., 2012). Most serum cortisol is bound to proteins, including corticosteroid-binding globulin and serum albumin (Perogamvros et al., 2011a,b), with both free and total concentrations varying diurnally. Free concentrations are between 10 and 300 nM (Lewis et al., 2005; Levine et al., 2007). Free cortisol passes easily through cellular membranes into the cytosol, where it can be converted to the inactive form—cortisone—or bind to intracellular cortisol receptors and reach the nucleus (Fig. 1). The anti-inflammatory effect and metabolism of cortisol on liver have not been studied extensively in vitro.

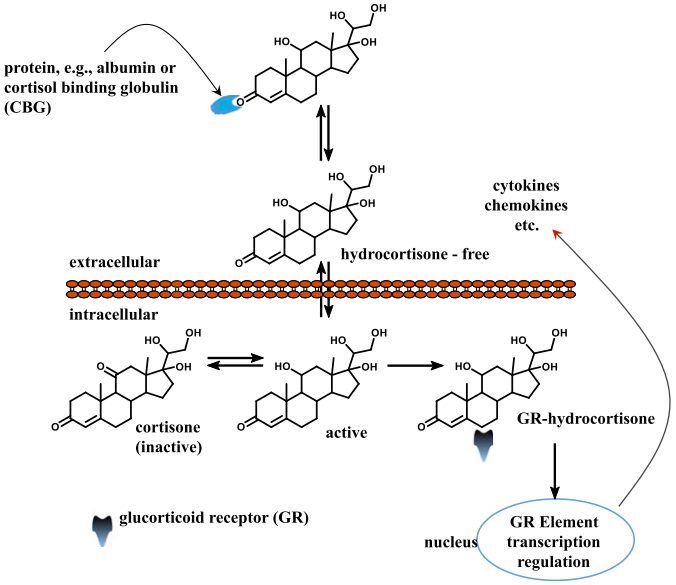

Fig. 1. Diffusion of cortisol to the nucleus. Cortisol is the most common glucocorticoid and is essential for life. It supports and regulates cardiovascular, metabolic, immunologic, and homeostatic functions.

Here, we introduce a cryopreserved primary human hepatocyte and Kupffer cell inflammatory liver model in which the cells are cultured in direct contact on an engineered scaffold recapitulating the liver capillary bed under perfusion (Fig. 2) (Powers et al., 2002a; Domansky et al., 2010). The model is used to examine the anti-inflammatory effect of glucocorticoids on liver cultures and, in conjunction with a sensitive and specific reversed-phase (RP)–ultra high-performance liquid chromatography (UHPLC)–quadrupole time of flight (QTOF)–mass spectrometry (MS) method, to study the metabolism of hydrocortisone at near-physiologic levels. The distribution of metabolites is compared with that in human urine.

Materials and Methods

Deuterated hydrocortisone (DLM-2218-0), used as an internal standard, was from Cambridge Isotope Laboratories (Tewksbury, MA). High-performance liquid chromatography–grade (≥99.9%) methanol (Chemical Abstract Service (CAS): 67-56-1), chloroform (CAS: 67-66-3), acetonitrile (ACN) (CAS: 75-05-8), formic acid (FA), (CAS: 64-18-6), molecular biology–grade dimethylsulfoxide (CAS: 67-68-5), dexamethasone (CAS: 50-02-2), hydrocortisone (CAS: 50-23-7), and 17-α-hydroxy-3,20-dioxopregn-4-en-21-yl-β-D-glucuronide were purchased from Sigma-Aldrich (St. Louis, MO). Calibration/tuning standard for the QTOF was from Agilent Technologies (Santa Clara, CA). The Oasis HLB cartridges were from EMD Millipore Corporation (Billerica, MA). Distilled water and acetonitrile were prepared in house with double distillation.

Coculture in the LiverChip. Cryopreserved human hepatocytes and human Kupffer cells were purchased from Life Technologies (Paisley, UK). Cells were thawed according to the instructions provided by the supplier. Viability was assessed using the trypan blue exclusion test (Strober, 2001) and was >85% for all lots.

Cells were seeded into LiverChip platforms (CNBio Innovations, Welwyn Garden City, Hertfordshire, UK) (Fig. 2A) housed in a humidified cell culture incubator at 37°C with 5% CO_2. The LiverChip platforms consist of 12 fluidically isolated bioreactors in which fluid is recirculated by a pneumatically driven micropump controlled by LiverChip hardware (Fig. 2B) through a scaffold containing cells (Fig. 2C). The scaffold enables the formation of an array of three-dimensional (3D) microtissues composed of either hepatocytes alone or hepatocytes in coculture with nonparenchymal cells (Kupffer cells) (Domansky et al., 2010). The platform is covered with a single loose lid, as per a standard microtiter plate enabling access to each of the 12 bioreactors for cell

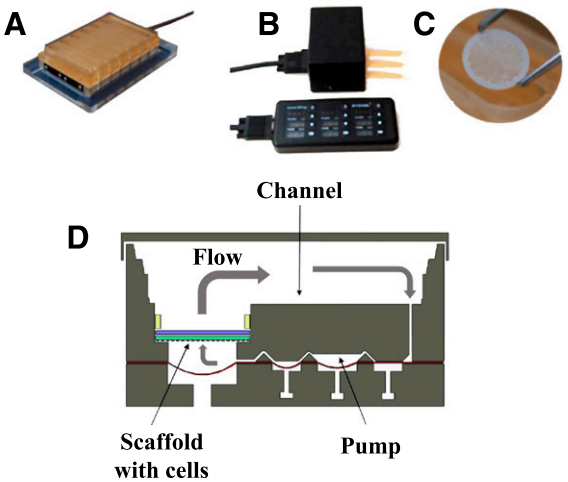

Fig. 2. Microfluidic 3D tissue culture system. (A) LiverChip. This device is a multiwell plate platform that enables maintenance of 3D liver tissue cultures under perfusion. (B) LiverChip hardware. (C) Scaffold containing 301 channels in which cells are seeded. Typically 0.6 × 106 human hepatocytes can be seeded per scaffold. (D) Schematic of flow through a single LiverChip culture well.

seeding, media change, and sampling. Each bioreactor can hold a maximum of 2.5 ml and has a surface channel which allows for efficient reoxygenation of the media by gaseous exchange with the atmosphere.

Cells were seeded with flow in the downward direction through the scaffold for 8 hours at a flow rate of 1.0 μl/s (Fig. 2D). Downward flow encourages cells to seed within the scaffold and form microtissues. Following cell attachment within the scaffold, the flow was changed to the upward direction and maintained at 1.0 μl/s for the remainder of the culture.

Hepatocyte monocultures were seeded at a density of 0.6×10^6 viable cells in 1.6 ml of medium per well. The cells were maintained in Williams' E medium (WEM) containing primary hepatocyte thawing and plating supplements (Life Technologies) for the first 24 hours of culture and in WEM containing primary hepatocyte maintenance supplements thereafter for the duration of the culture.

Hepatocyte and Kupffer cell cocultures were seeded simultaneously, maintaining the same number of hepatocytes while adjusting the number of Kupffer cells to achieve the desired ratios of hepatocytes:Kupffer cells (Supplemental Table 1). Cocultures were seeded in WEM containing primary human hepatocyte thawing and plating supplements for the first 24 hours of culture, and then in WEM with primary human hepatocyte maintenance supplements. On day 3, for both mono- and cocultures, where appropriate, hydrocortisone (100 nM) was substituted for 100 nM dexamethasone, and the medium was changed every 48 hours. To induce an inflammatory state in the cultures, LPS (Sigma-Aldrich, Poole, UK) was added in the culture medium.

Total Protein. Cells and scaffolds were washed once in phosphate-buffered saline and lysed using 0.5 ml of 0.1 M NaOH containing 2% SDS. Total cellular protein was then measured with a Pierce BCA protein assay kit (Thermo Fisher, Loughborough, UK).

Hepatocyte and Kupffer Cell Phenotyping. Albumin secretion was measured with a human albumin enzyme-linked immunosorbent assay (Assay Pro, St. Charles, MO). Urea was quantified with a colorimetric assay kit (BioAssay Systems, Hayward, CA). Interleukin 6 (IL6) and tumor necrosis factor α (TNFα) production were quantified in culture medium using human DuoSet kits (R&D Systems, Abingdon, UK).

CYP3A Activity. CYP3A activity was measured with the P450-Glo CYP3A4 assay with Luciferin-IPA (Promega, Southampton, UK). A complete medium change to medium containing a 1000-fold dilution of Luciferin-IPA was performed and the plate returned to the incubator with flow. After 1 hour, 50 μl from each well was placed in an opaque 96-well assay plate, and 50 μl of the luciferin detection reagent was added. The plate was incubated at room temperature for 20 minutes, protected from the light, and luminescence measured relative to a standard curve of beetle luciferin potassium salt (Promega).

Metabolite Extraction. Frozen samples for an analytical series were thawed at the same time and kept on ice. Unused samples were then immediately stored at −80°C. A stock solution of 1.25 μM d_4-hydrocortisone (d_4-HC) was prepared, and 2 μl was spiked into a 50-μl sample for a final concentration of 50 nM. The samples were incubated in ice for 2 minutes after adding cold methanol and cold chloroform (high-performance liquid chromatography grade) at a 1:1:4 ratio relative to sample volume. After vortexing for 20 seconds and shaking for another 5 minutes, the samples were incubated at −20°C for 30 minutes. Subsequently, the samples were again vortexed for 20 seconds followed by centrifugation at 15,000 rpm for 10 minutes. The organic phase was collected carefully with a special narrow gel tip (Bioscience, Inc., Salt Lake City, UT) and dried in a SpeedVac SC110 (Savant Instruments, Holbrook, NY). Samples were immediately prepared for liquid chromatography-mass spectrometry (LC-MS) by resuspending in 50 μl of 2% ACN containing 0.1% formic acid.

Preparation of Standards for Calibration Curves. Hydrocortisone was dried overnight under vacuum to remove any residual water. Distilled water was used to prepare different concentrations of HC (e.g., 2, 5, 10, and 20 μM) and verify the accurate concentration of a working stock solution by UV absorption. The concentration of each HC solution was determined by UV at 242 nm with ε = 16,000 as the molar extinction coefficient.

LC-MS standards were prepared by diluting the working stock solution with Williams' E medium to give concentrations of 5, 10, 50, 75, 100, and 200 nM. All LC-MS standards and stock solutions were stored at 4°C and allowed to equilibrate at room temperature for at least 15 minutes before use. For calibration, a 50-μl aliquot of each LC-MS standard was spiked with 2 μl of the 1.25 μM d_4-HC internal standard solution, and the metabolites were extracted as previously described. Samples for LC-MS analyses were immediately resuspended in 50 μl of 2% ACN containing 0.1% formic acid. The calibration curve was constructed by plotting the peak area ratios of hydrocortisone relative to those of d_4-HC against the concentrations (nanomolar) of the LC-MS standards.

LC-MS Parameters and Metabolite Profiling. The method validations are described in the Supplemental Method. LC-MS analyses were performed on an Agilent 6530 Accurate-Mass LC-QTOF mass spectrometer with an Agilent Jet Stream electrospray ionization source and MassHunter workstation (version B.06). The mass spectrometer was interfaced with an Agilent 1290 ultra performance liquid chromatography system. The column was an Agilent Extend-C18 (2.1 × 50 mm, 1.8 μm). The column compartment temperature was set at 40°C. The QTOF was calibrated daily using the standard tuning solution from Agilent Technologies. The mass spectra were acquired in positive ion mode for total and free hydrocortisone measurements and in negative ion mode for the analysis of glucuronides. Mass spectra were collected between *m/z* 70 and 1000 at either 2 or 4 scans/s. The ion spray voltage was set at 3800 V, the heated capillary temperature was 350°C, drying gas was 8 l/min, nebulizer was 30 psi, sheath gas temperature was set at 380°C, and sheath gas flow was 12 l/min. Two reference masses (*m/z* 121.0509: $C_5H_4N_4$; *m/z* 922.0098: $C_{18}H_{18}O_6N_3P_3F_{24}$) were continuously infused to allow mass correction during the run. Tandem mass spectrometry (MS/MS) spectra were typically obtained at a collision energy of 20 eV. Variations of retention times and *m/z* values were ≤0.2 minute and 10 mDa, respectively, and the relative standard deviations of peak areas were below 20%, indicating good reproducibility and stability of the chromatographic separation and mass accuracy during a sequence (typically over 100 runs). The mobile phases were double-distilled water containing 0.1% formic acid (A) and distilled acetonitrile containing 0.1% formic acid (B). A linear gradient was run from 2 to 95% B over 12 minutes at 0.4 ml/min.

Data Processing. Hydrocortisone disappearance was followed on the QTOF in MS mode. Data were processed using Agilent MassHunter qualitative analysis software (version B.06). Peak areas of HC (*m/z* 363.2171), d_4-HC (*m/z* 367.2423), and dexamethasone (*m/z* 393.2077) were obtained using the extracted ion chromatogram function. Hydrocortisone and metabolites data were analyzed both manually and using the molecular feature extractor, i.e., all signals associated with a given analyte, with intensities >1000, were used to profile metabolites, with a 10-ppm mass accuracy threshold. The data were further processed using Excel 2011 (Microsoft, Redmond, WA), and quantification was based on calibration curves built with known concentrations of hydrocortisone standards. GraphPad Prism software (GraphPad, La Jolla, CA) was used to plot the data using the means of biologic replicates with corresponding relative standard deviations.

Targeted MS/MS spectra, via matched exact masses and associated retention times, were generated on the Agilent QTOF 6530 mass spectrometer to support the identities of the metabolites, followed by metabolic pathway or function analysis with the Kyoto Encyclopedia of Genes and Genomes database (http://www.genome.jp/kegg/; http://metlin.scripps.edu/index.php). The MS/MS spectra were also analyzed with the Agilent molecular structure correlator, which compares the accurate mass of the MS/MS fragment ions for a compound of interest with one or more proposed structures for that compound.

Analysis of Glucuronides. LC-MS analyses of glucuronides were also performed on the Agilent 6530 mass spectrometer. Conditions for calibration and sample analyses were the same as those for metabolite profiling by LC-MS except that the negative ion mode was used. Five microliters of the glucuronide internal standard solution was added to a 50 μl aliquot of the bioreactor culture medium to make a final concentration of 50 nM 17-α-hydroxy-3,20-dioxopregn-4-en-21-yl-β-D-glucuronide, and the mixture was then diluted with 100 μl of 5 mM ammonium acetate buffer (pH 5). The samples were thoroughly mixed and then applied to an Oasis HLB cartridge (10 mg, 1 ml) after washing the cartridges with methanol (1 ml) and water (1 ml). The cartridges were then washed with water (1 ml) to remove unbound material, and

the glucuronides eluted with methanol (1 ml). The samples were then dried in a SpeedVac and immediately resuspended in 25 μl of water with 2% ACN and 0.1% formic acid.

Estimation of In Vitro Hydrocortisone Pharmacokinetic Parameters. Hydrocortisone pharmacokinetics parameters were calculated using the following equations (eqs. 1–4), where $t_{1/2}$ is the half-life, k_{el} is the rate of elimination, CL is the clearance, V_d is the volume of distribution, AUC is the area under the curve, t is time, and C is concentration. The V_d of the system was 2.2 ml:

$$t_{1/2} = \frac{\text{time elapsed} * 0.30103}{\log \frac{\text{first point}}{\text{second point}}} \quad (1)$$

$$k_{el} = \frac{\ln 2}{t_{1/2}} \quad (2)$$

$$CL = V_d * k_{el} \quad (3)$$

$$AUC = (t_1 - t_2) * \frac{C_1 + C_2}{2} \quad (4)$$

Measurements of Unbound (Free) Hydrocortisone. A fast ultra performance liquid chromatography–MS/MS method was developed to analyze free HC without sample preparation. The LC parameters were the same as previously described. The switching valve of the Agilent 6530 Accurate-Mass LC- QTOF mass spectrometer was used to divert salt content to waste from 0 to 2.7 minutes and high protein content from 4 to 13 minutes (the HC elutes at 3.4 minutes). Two different samples were analyzed: 1) hepatocyte and Kupffer cell cocultures at time zero containing 100 nM HC and 1.25 mg/ml human serum albumin (HSA), and 2) hepatocyte and Kupffer cell cocultures at time zero containing 100 nM HC and 25 mg/ml HSA. The injection volume was limited to 1 μl to avoid overloading the column.

Results

Coculture Model Characterization. Several ratios (Supplemental Table 1) of human cryopreserved hepatocytes and human cryopreserved Kupffer cells, i.e., 15:1 (low inflammation), 10:1 (moderately inflamed), and 2.5:1 (highly inflamed), were cultured in the microbioreactor platform and assessed over an 8-day period. The cell health and differentiated state of the primary human hepatocytes maintained over 8 days in the bioreactor were monitored. Finally, LPS was introduced to the cultures to elicit an inflammatory response, as assessed by the release of proinflammatory cytokines, IL6, and TNFα via sandwich enzyme-linked immunosorbent assays.

Phase contrast imaging (Ti-Eclipse; Nikon, Tokyo, Japan) was used to visualize the morphology of the tissue formation within the scaffold after 8 days in culture. Figure 3 shows the tissue formation in mono- and 10:1 cocultures; no change in microtissue structure is observed as a result of the addition of Kupffer cells. CYP3A activity and total protein levels were measured at day 8

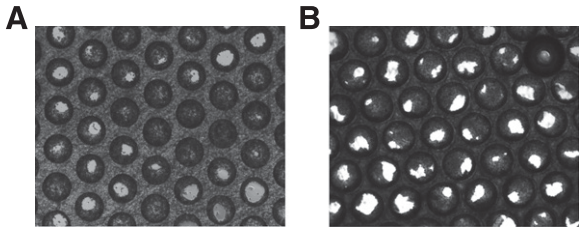

Fig. 3. Tissue formation. Phase-contrast imaging (Ti-Eclipse; Nikon) was used to assess the morphology of the tissue formation after 7 days in culture. (A) Monoculture. (B) Coculture plated at 10:1 cell type ratio.

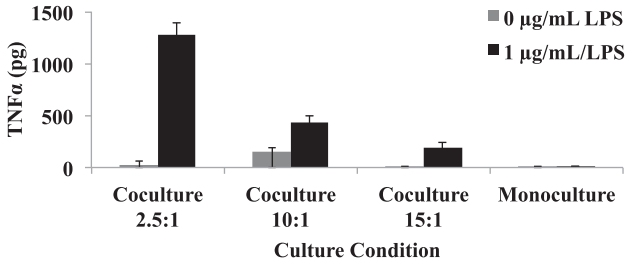

Fig. 4. Inflammation stimulated by the addition of 1 μg/ml LPS to the monoculture and coculture systems seeded at 2.5:1, 10:1, and 15:1 ratios. TNFα was measured as a marker of Kupffer cell activation (n = 3 replicates, single donor). Results are reported as the mean ± S.D.

(Supplemental Fig. 1). No significant differences were observed between the four conditions, demonstrating that the addition of Kupffer cells did not adversely affect cell health or inhibit the CYP3A activity in LPS naïve cultures. The albumin production rates after 8 days in culture were greater than 30 μg/mg total protein/day for all conditions, a level similar to human in vivo production (Supplemental Fig. 1).

To assess the functionality of the Kupffer cells in cocultures with hepatocytes, cultures were exposed to LPS (1 μg/ml) for 48 hours starting on day 6 (Fig. 4). TNFα was measured as a marker of Kupffer cell activation. In LPS naïve cultures, the TNFα concentration was ~19 pg/ml after a 48-hour period. The addition of LPS caused increased secretion of TNFα into the culture medium. The level of production of cytokines was dependent on the number of Kupffer cells seeded in the culture. The highest ratio of hepatocytes to Kupffer cells (2.5:1) resulted in a 42-fold increase in TNFα production in comparison with 15:1, which induced a 32-fold increase in production. Before stimulation, the Kupffer cells were relatively quiescent but clearly remained viable and responsive to the addition of supraphysiologic levels of LPS. IL6 production followed similar trends upon LPS stimulation. Stimulation of monocultures resulted in undetectable levels of cytokines in the media, confirming Kupffer cells are responsible for cytokine production, and the cryopreserved human hepatocyte lots used in this study are uncontaminated with residual amounts of Kupffer cells (data not shown).

Anti-inflammatory Capacity of Coculture in Response to Endogenous and Synthesized Glucocorticoids. Hydrocortisone, a human endogenous glucocorticoid, has anti-inflammatory properties. Cocultures were exposed to various concentrations of hydrocortisone (0, 100, and 500 nM) up to day 7 in culture. To assess the effects of these concentrations, cytokine production was measured after the addition of 1 μg/ml LPS for 24 hours. As expected, in LPS naïve culture, low levels of TNFα and IL6 were detected (Supplemental Fig. 2). Cultures without hydrocortisone produced the highest levels of cytokines, with 1350 and 1043 pg for TNFα and IL6, respectively. The addition of 100 and 500 nM hydrocortisone caused a decrease in TNFα to 355 and 191 pg, respectively. Similar trends were observed for IL6.

To determine if the model has utility as a platform to screen anti-inflammatory compounds, the anti-inflammatory effects of hydrocortisone and dexamethasone were assessed at 100 nM (Supplemental Fig. 3). After dosing with either hydrocortisone or dexamethasone from day 3 to 7, the cultures were stimulated with 1 μg/ml LPS for 24 hours. Hydrocortisone showed a modest anti-inflammatory effect, whereas dexamethasone showed a greater reduction in the levels of both TNFα and IL6.

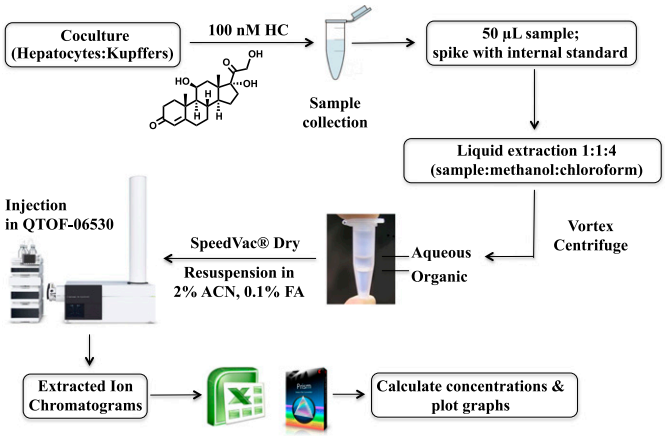

Fig. 5. Experimental workflow used for the quantification of hydrocortisone as metabolite profiling. The method consists of spiking with internal standard, liquid extraction, and mass spectrometry analysis.

Experimental Workflows. Figure 5 shows the experimental workflow for the quantification of hydrocortisone and metabolite profiling. The protocol is described in detail in *Materials and Methods*; in brief, samples were spiked with internal standard, extracted with methanol and chloroform, dried, and analyzed using RP-UHPLC-QTOF-MS. The aqueous layer was analyzed to confirm that there was no loss of hydrocortisone during the extraction process (Supplemental Fig. 4). For the analysis of the glucuronides (Supplemental Fig. 5), the samples were solid phase extracted in an Oasis HLB, then dried in a SpeedVac and analyzed using RP-UHPLC-QTOF-MS.

Hydrocortisone Clearance. Cocultures were seeded in LiverChip in duplicate to estimate biologic variability within the bioreactor wells. Each well was treated with 100 nM hydrocortisone, and culture media samples collected at 0, 24, and 48 hours were analyzed. Variation from technical sources, such as pipetting and liquid extraction, was assessed. Each well was extracted two times, and each extraction was run twice consecutively in positive ion mode in RP-UHPLC-QTOF-MS (Supplemental Fig. 6). A concern in drug clearance studies in bioreactors is whether the drug is adsorbed onto any of the materials used in the apparatus. Two other wells without cells were therefore used as controls for nonspecific binding experiments, using the same drug dose, sample collection, and analysis. The concentration of hydrocortisone was virtually constant over a period of 4 hours, i.e., any loss of HC during coculture experiments can be attributed to cellular metabolism (Supplemental Fig. 7).

Hydrocortisone disappearance in the bioreactor is plotted in Fig. 6. Under noninflamed conditions, 100 nM hydrocortisone was depleted to approximately 30 nM in the culture medium after 48 hours.

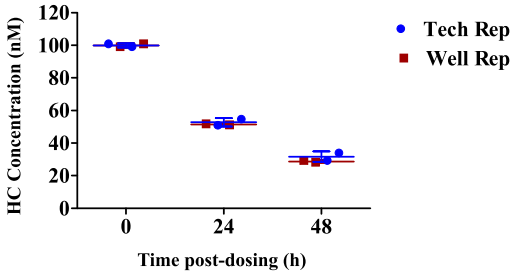

Fig. 6. Hydrocortisone disappearance over time (n = 2 for biologic and technical replicates). Lines represent the mean ± S.D.

A logarithmic plot (ln HC/HC_0) versus time postdosing (Supplemental Fig. 8) indicates that the clearance of HC follows first-order kinetics.

Donor-to-Donor Variability. Hepatocytes and Kupffer cells from three different donor pairs (Supplemental Table 2) were plated as cocultures under noninflamed conditions and treated with 100 nM hydrocortisone. The assessment was made by comparing the HC disappearance rates of each of the donors (Supplemental Fig. 9). The percent relative standard deviation was ≤15%, confirming that the donor-dependent variability in HC clearance rates in the 3D microbioreactor platforms is acceptably low.

Effect of LPS on HC Clearance Rate. Lipopolysaccharide is a component of Gram-negative bacterial cell walls and is associated with tissue injury and sepsis. To further unravel the mechanisms underlying inflammatory reactions in the liver, hepatocytes were plated in duplicate as cocultures with Kupffer cells at a 10:1 ratio, and the media were changed on day 4 to fresh media containing 100 nM HC with LPS at concentrations of 0, 0.1, and 1 μg/ml. Culture media samples were collected at 0, 24, and 48 hours. The media were then replaced on day 6 with fresh media containing 100 nM HC and LPS and samples taken on day 8. For technical variation assessment, each replicate was extracted twice, and each of the two extracts was run in positive ion mode in the RP-UHPLC-QTOF-MS two times consecutively. HC concentrations in the bioreactor were plotted versus time (Supplemental Fig. 10). The rates are equivalent in every case when comparing noninflamed cocultures with LPS-induced cocultures, suggesting that inflammation neither inhibited nor induced the activity of reductases involved in the metabolism of hydrocortisone in the bioreactors. The HC clearance rates from day 5 to 7 were similar to those from day 3 to 5, indicating that extended exposure to LPS did not affect clearance (data not shown).

Hydrocortisone Metabolism: Phase I/II Metabolites. High-accuracy exact mass, retention time, and database searching, followed by manual interpretation of collision-induced dissociation MS/MS spectra, were used to confirm the structures of the hydrocortisone metabolites. The MS/MS spectra revealed a characteristic fragmentation pattern with ions at m/z 267.1747, 121.0650, and 163.1119. For example, the MS/MS spectrum of cortisone, which is the oxidized product of hydrocortisone, showed the m/z 163.1119 fragment as the most intense and characteristic ion, which is not found in the MS/MS spectrum of hydrocortisone (Supplemental Fig. 11).

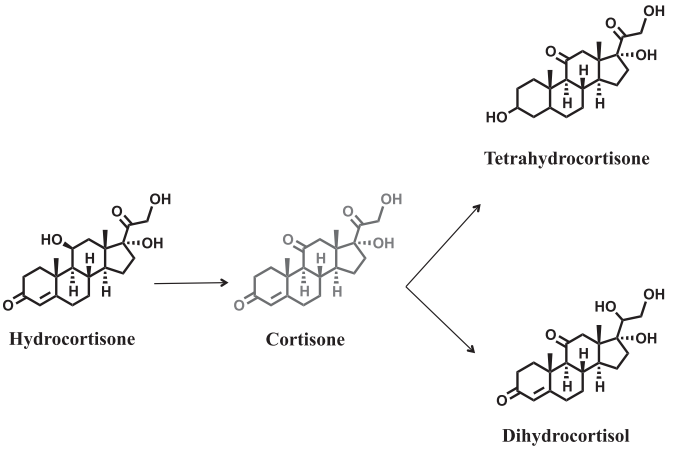

Fig. 7. Phase I metabolites. A total of 8–10% of hydrocortisone was found as phase I metabolites, including tetrahydrocortisone and dihydrocortisol.

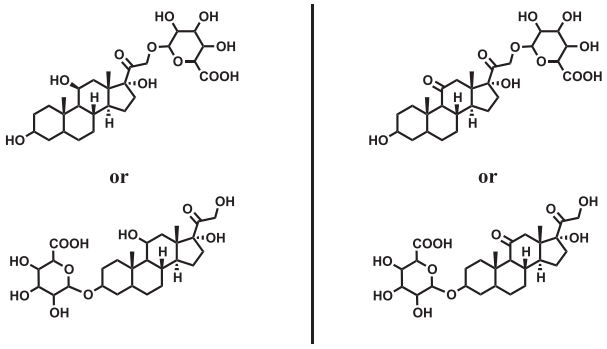

Fig. 8. Phase II metabolites. A total of 45–52% of hydrocortisone was found as phase II metabolites, including tetrahydrocortisol glucuronide and tetrahydrocortisone glucuronide.

As noted earlier (Fig. 6), approximately 70% of the hydrocortisone disappeared over 48 hours, and this was largely accounted for as 8% phase I metabolites and 52% phase II metabolites. In the absence of authentic standards, tetrahydrocortisone, dihydrocortisol (phase I; Fig. 7) and tetrahydrocortisol, and tetrahydrocortisone glucuronides (phase II; Fig. 8) were confirmed by comparing their retention times, exact monoisotopic masses, and MS/MS spectra with those of known hydrocortisone metabolites found in human urine (Supplemental Figs. 12 and 13).

Hydrocortisone Pharmacokinetics. The pharmacokinetics of hydrocortisone were investigated after administration of 100 nM HC to a coculture of human hepatocytes and Kupffer cells in the bioreactor. The HC concentrations in culture media were measured by LC-MS/MS, and the pharmacokinetics were determined using standard pharmacokinetic equations (eqs. 1–4).

The mean culture media concentration-time curve after administration of 100 nM hydrocortisone is shown in Fig. 6. The $t_{1/2}$, k_{el}, hydrocortisone CL, and AUC were estimated to be 23.03 hours, 0.03 hour^{1}, 6.6×10^{-5} l·hour^{-1}, and 1.03 (mg/l)*h, respectively (see also Table 1).

Albumin is the most abundant plasma protein, with a half-life of 3 weeks (Peters, 1970). Some drug molecules are rapidly excreted from the circulation, resulting in lower therapeutic efficacies. In this regard, albumin plays a role in increasing plasma half-life through noncovalent interaction with the small molecules (Sleep et al., 2013). Protein-drug binding may affect pharmacokinetic behaviors, including the half-life of a drug (Tayman et al., 2011). It is interesting to see whether protein concentration may show a similar effect in the 3D microbioreactors. To test this hypothesis, we used a higher concentration of human serum albumin (25 mg/ml) and analyzed the HC clearance. The half-life calculated for high protein concentration was higher in comparison with 1.25 mg/ml HSA ($t_{1/2}$ = 34.36 hours vs. $t_{1/2}$ = 23.03 hours), indicating that the number of available interactions with the HC extended the half-life. Hydrocortisone was 50% bound with 25 mg/l albumin, and almost all free with 1.25 mg/ml albumin. The fraction unbound (f_u) was expressed using eq. 5, where [D] is the free drug concentration and [DP] is the concentration of drug protein complex:

$$f_u = \frac{[D]}{[D] + [DP]} \tag{5}$$

TABLE 1

Pharmacokinetic parameters obtained after administration of 100 nM hydrocortisone to a coculture of human hepatocytes and Kupffer cells in the human liver bioreactor

Symbol	Characteristic	Value	Unit
$t_{1/2}$	Elimination half-life	23	h
k_{el}	Elimination rate constant	0.03	h^{-1}
V_d	Volume of distribution	2.2	ml
CL	Clearance	6.6×10^{-5}	$l \cdot h^{-1}$
AUC	Area under the curve	1.03	$\frac{mg}{l} * h$

Extrapolation of In Vivo Intrinsic Clearance of Hydrocortisone from In Vitro Data. The prediction of human clearance is a key objective in drug discovery. It is therefore important to establish an in vitro/in vivo correlation (IVIVC) for the clearance of hydrocortisone based on in vitro metabolism data. For this, in vitro data from the 3D microbioreactor were used to estimate expected in vivo data that could be compared with the in vivo clearance in humans. The in vitro half-life was used to calculate the in vitro intrinsic clearance using the scaling factors in eq. 6:

$$CL_{int} = \frac{\ln 2}{t_{1/2}} * \frac{\text{liver weight}}{\text{standard body weight}} * \frac{\text{incubation volume}}{\text{hepatocytes/well}} * \text{hepatocytes/g liver} \tag{6}$$

Scaling parameters were used for the calculations (Supplemental Table 3) (Davies and Morris, 1993; Obach et al., 1997). The hepatic clearance (CL_h) was calculated from intrinsic clearance (CL_{int}) using the well-stirred model (eq. 7) (Pang and Rowland, 1977a,b). CL_h was calculated for hydrocortisone, correcting for the plasma protein binding ($f_{u\ b}$) from the literature (Robin et al., 1978) and using eq. 7, where Q is the hepatic blood flow rate and $f_{u\ inc}$ is the unbound fraction in hepatocytes from the bioreactor. To compare in vivo intrinsic clearance values with in vitro in vivo clearance values, eq. 7 was rearranged into eq. 8 (Davies and Morris, 1993; Bayliss et al., 1999; Chiba et al., 2009; Chan et al., 2013):

$$CL_h = \frac{Q * f_{u\ b} * \left(\frac{CL_{int}}{f_{u\ inc}}\right)}{Q + \left[f_{u\ b} * \left(\frac{CL_{int}}{f_{u\ inc}}\right)\right]} \tag{7}$$

$$CL_{int-in\ vivo} = \frac{Q * CL_h}{(Q - CL_h) * f_{u\ b}} \tag{8}$$

The CL_{int} calculated by eq. 6 was 5.7 ml/min/kg, and the hepatic clearance was 1.1 ml/min/kg (assuming f_u = 1). The in vivo clearance data from LiverChip calculated in milliliters per minute per kilogram were converted to liters per hour using the human body weight (average body weight = 70 kg). The in vivo intrinsic clearance ($CL_{int\text{-}in\ vivo}$) was calculated to be 23.8 l/h, which is 1.3-fold higher than human in vivo clearance, i.e., approximately 18 l/h (Derendorf et al., 1991).

Discussion

Multiple approaches aimed at halting the relatively rapid de-differentiation of primary hepatocytes in monolayer in vitro cultures have been studied. Coculturing of hepatocytes with feeder or liver nonparenchymal cells (NPCs) has proved effective, as has 3D culture

in various formats, including bioreactors. Work in this area typically focuses on maintenance of hepatic viability and function with relatively less emphasis placed on deploying the models to explore disease states such as inflammation or in concert with high-quality analytics to produce detailed pharmacokinetic information. A notable exception is the micropattern cocultures first published by Khetani and Bhatia (2006, 2008), which have been used for extensive clearance and metabolite identification studies (Wang et al., 2010; Dash et al., 2012; Chan et al., 2013). Here we demonstrate an inflammatory liver model supported in a 3D bioreactor culture system to explore the metabolism and anti-inflammatory effects of hydrocortisone.

We developed 3D cultures of primary hepatocytes and a mixed fraction of liver NPCs, as unsupported spheroids and in scaffold-containing bioreactors have been shown to maintain hepatic viability and produce proinflammatory cytokines on stimulation with high concentrations of LPS (Dash et al., 2009; Messner et al., 2013). The NPCs in these models likely play a dual role, both supporting hepatic function and recapitulating inflammatory response. In the model described here, a modular approach starting from separate stocks of cryopreserved human hepatocytes and Kupffer cells has been taken. The bioreactor and 3D scaffold are sufficient to maintain hepatocyte viability for extended periods in the presence or absence of NPC (Powers et al., 2002b; Sivaraman et al., 2005; Vivares et al., 2015). Kupffer cells can therefore be added to the cultures in well defined ratios, allowing the evaluation of models of noninflamed, mild, and highly inflamed livers with ratios of hepatocytes to Kupffer cells ranging from 15:1 to 2.5:1.

Glucocorticoids are necessary in the media of primary hepatocyte cultures, as they assist in the preservation of the differentiated state as reflected, e.g., by the maintenance of cytochrome P450 levels (Schuetz et al., 1984; Schuetz and Guzelian, 1984). In the media for Kupffer cell monocultures, glucocorticoids are removed or kept at low nanomolar concentrations, as their presence blunts cytokine production. Hydrocortisone, or cortisol, is the major human glucocorticoid; here, we confirm that hepatocyte and Kupffer cell cocultures can be maintained in hydrocortisone-containing media, and that hydrocortisone shows a dose-dependent anti-inflammatory effect. When compared with hydrocortisone at 100 nM, dexamethasone has a more potent anti-inflammatory effect as judged by suppression of cytokine production, reflecting the situation in vivo.

The metabolism of hydrocortisone has not been extensively investigated in vitro in 3D perfusion models, particularly at concentrations near physiologic free levels. To exemplify the utility of the model not only for anti-inflammatory drug testing but also for complex drug metabolism studies, a detailed characterization of hydrocortisone disappearance and metabolite profile has been undertaken. For metabolism studies of hydrocortisone, an initial concentration of 100 nM was used. The hydrocortisone was depleted to 30 nM after 48 hours, with first-order kinetics. LC-MS approaches were used to identify the metabolites produced in the bioreactor; tetrahydrocortisone and dihydrocortisone were identified as major and minor phase I metabolites, respectively. The majority of the metabolism, however, was glucuronidation; phase II metabolites were identified as tetrahydrocortisol glucuronide and tetrahydrocortisone glucuronides. Toward the end of the application period, the formation rates of tetrahydrocortisol glucuronide and tetrahydrocortisone glucuronide were higher than at earlier time points in the bioreactor cultures, suggesting that UDP-glucuronosyltransferase (Kaji and Kume, 2005) and other oxodoreductases (reductive enzymes) were present in the bioreactor cultures.

Donor-to-donor variability was assessed by comparing the HC disappearance rates of several donors. The donor-dependent variability is low, supporting the promise of this microphysiological system as a tool for investigating drug metabolism and anti-inflammatory effects (Supplemental Fig. 9).

To address whether the hydrocortisone nominal disappearance included a contribution from prior or metabolically formed cortisone, we used [9,11,12,12-$^{2}H_4$] hydrocortisone (d_4-hydrocortisone) as a tracer (Supplemental Fig. 14). The deuterated isotopomer can be distinguished from unlabeled hydrocortisone by the mass difference of 4 Da. Metabolism by the 11β-hydroxysteroid dehydrogenase type 2 enzyme would yield cortisone, with the deuterium at the 11β position being lost. The resulting [9,12,12-$^{2}H_3$] cortisone (d_3-cortisone) would have a mass 1 Da less than that of the d_4-hydrocortisone. Subsequent conversion of cortisone via 11β-hydroxysteroid dehydrogenase type1 back to hydrocortisone would yield d_3-hydrocortisone, which is 1 Da less than the starting isotopomers. Regeneration of d_4-hydrocortisone is unlikely since this would require reintroduction of highly diluted deuterium at the 11β position. The 1-Da mass difference and the contribution of the ^{13}C abundance of the d_4 compound to the signal from the presumed d_3-hydrocortisone preclude a detailed interpretation. There appears, however, to be some cortisone-hydrocortisone interconversion, although the net effect on hydrocortisone disappearance is modest at best.

To further understand the functionality of the Kupffer cells in cocultures with hepatocytes, the system was exposed to LPS for 48 hours to stimulate inflammation. The disappearance rate of hydrocortisone was not affected by stimulation of the cultures with LPS. We have demonstrated that hydrocortisone is primarily metabolized by phase II enzymes and hypothesize that this is the reason that LPS stimulation has little effect on clearance rate. LPS stimulation causes the release of proinflammatory cytokines, which are known to downregulate cytochrome P450 (Milosevic et al., 1999).

Pharmacokinetic parameters were estimated for the in vitro metabolism and to establish IVIVC of hydrocortisone behavior. The CL_{int} was ~5.7 ml/min/kg (calculated using eq. 6). Hepatic clearance was ~1.1 ml/min/kg (assuming f_u = 1), and the calculated value for $CL_{int\text{-}in\ vivo}$ was 23.8 l/h, which is 1.3 times that of human in vivo clearance (approximately 18 l/h) (Derendorf et al., 1991). The intrinsic clearance values and the metabolites generated in the perfused human 3D microbioreactor correlated generally with human data.

In summary, cytochrome P450 activities, total protein, albumin, and urea levels were maintained for extended periods of coculture in the microphysiological system, a useful tool for pharmacological or toxicological investigations requiring a highly stable and reproducible physiologic in vitro representation of the human liver.

We demonstrated the applicability of a recently developed bioreactor for long-term pharmacological investigations on a human hepatocyte coculture system, using hydrocortisone as a steroidal anti-inflammatory drug model. Correlations between in vitro and in vivo data (IVIVC) were generated, suggesting that 3D microphysiological systems with mixed human cell populations could be used as tools for investigating drug metabolism and toxicity for drug development.

Overall, the biology in the coculture system and the in vitro and in vivo hepatic clearance correlation data suggest that the roles of various uptake and efflux transporters in drug efficacy and toxicity studies in these systems may also correlate with the human liver in vivo.

Thus, especially if interactions with nonparenchymal cells are involved, the miniaturized bioreactor may be a useful model system to increase predictivity in pharmacological and toxicological studies on a subchronic timescale. In addition, the culture system facilitates histologic analyses of pharmacology-related structural characteristics of human liver tissue.

Acknowledgments

The authors thank Agilent Technologies for access to the triple quadrupole mass spectrometer.

Authorship Contributions

Participated in research design: Sarkar, Rivera-Burgos, Large, Hughes, Ravindra, Ebrahimkhani, Wishnok, Griffith, Tannenbaum.

Conducted experiments: Sarkar, Rivera-Burgos, Large, Ravindra, Dyer.

Performed data analysis: Sarkar, Rivera-Burgos, Large, Ravindra, Wishnok, Tannenbaum.

Wrote or contributed to the writing of the manuscript: Sarkar, Rivera-Burgos, Large, Hughes, Ravindra, Griffith, Wishnok, Tannenbaum.

References

Adams DH, Ju C, Ramaiah SK, Uetrecht J, and Jaeschke H (2010) Mechanisms of immune-mediated liver injury. *Toxicol Sci* **115**:307–321.

Baffet G, Clément B, Glaise D, Guillouzo A, and Guguen-Guillouzo C (1982) Hydrocortisone modulates the production of extracellular material and albumin in long-term cocultures of adult rat hepatocytes with other liver epithelial cells. *Biochem Biophys Res Commun* **109**: 507–512.

Bayliss MK, Bell JA, Jenner WN, Park GR, and Wilson K (1999) Utility of hepatocytes to model species differences in the metabolism of loxtidine and to predict pharmacokinetic parameters in rat, dog and man. *Xenobiotica* **29**:253–268.

Chan TS, Yu H, Moore A, Khetani SR, and Tweedie D (2013) Meeting the challenge of predicting hepatic clearance of compounds slowly metabolized by cytochrome P450 using a novel hepatocyte model, HepatoPac. *Drug Metab Dispos* **41**:2024–2032.

Chiba M, Ishii Y, and Sugiyama Y (2009) Prediction of hepatic clearance in human from in vitro data for successful drug development. *AAPS J* **11**:262–276.

Cosgrove BD, King BM, Hasan MA, Alexopoulos LG, Farazi PA, Hendriks BS, Griffith LG, Sorger PK, Tidor B, and Xu JJ, et al. (2009) Synergistic drug-cytokine induction of hepatocellular death as an in vitro approach for the study of inflammation-associated idiosyncratic drug hepatotoxicity. *Toxicol Appl Pharmacol* **237**:317–330.

Dash A, Blackman BR, and Wamhoff BR (2012) Organotypic systems in drug metabolism and toxicity: challenges and opportunities. *Expert Opin Drug Metab Toxicol* **8**:999–1014.

Dash A, Inman W, Hoffmaster K, Sevidal S, Kelly J, Obach RS, Griffith LG, and Tannenbaum SR (2009) Liver tissue engineering in the evaluation of drug safety. *Expert Opin Drug Metab Toxicol* **5**:1159–1174.

Davies B and Morris T (1993) Physiological parameters in laboratory animals and humans. *Pharm Res* **10**:1093–1095.

Deng X, Liguori MJ, Sparkenbaugh EM, Waring JF, Blomme EA, Ganey PE, and Roth RA (2008) Gene expression profiles in livers from diclofenac-treated rats reveal intestinal bacteria-dependent and -independent pathways associated with liver injury. *J Pharmacol Exp Ther* **327**: 634–644.

Deng X, Luyendyk JP, Ganey PE, and Roth RA (2009) Inflammatory stress and idiosyncratic hepatotoxicity: hints from animal models. *Pharmacol Rev* **61**:262–282.

Derendorf H, Möllmann H, Barth J, Möllmann C, Tunn S, and Krieg M (1991) Pharmacokinetics and oral bioavailability of hydrocortisone. *J Clin Pharmacol* **31**:473–476.

Domansky K, Inman W, Serdy J, Dash A, Lim MH, and Griffith LG (2010) Perfused multiwell plate for 3D liver tissue engineering. *Lab Chip* **10**:51–58.

Drewitz M, Helbling M, Fried N, Bieri M, Moritz W, Lichtenberg J, and Kelm JM (2011) Towards automated production and drug sensitivity testing using scaffold-free spherical tumor microtissues. *Biotechnol J* **6**:1488–1496.

Godoy P, Lakkapamu S, Schug M, Bauer A, Stewart JD, Bedawi E, Hammad S, Amin J, Marchan R, and Schormann W, et al. (2010) Dexamethasone-dependent versus -independent markers of epithelial to mesenchymal transition in primary hepatocytes. *Biol Chem* **391**: 73–83.

Groothuis GM and Meijer DK (1992) Hepatocyte heterogeneity in bile formation and hepatobiliary transport of drugs. *Enzyme* **46**:94–138.

Guengerich FP (2011) Mechanisms of drug toxicity and relevance to pharmaceutical development. *Drug Metab Pharmacokinet* **26**:3–14.

Guillouzo A, Delers F, Clement B, Bernard N, and Engler R (1984) Long term production of acute-phase proteins by adult rat hepatocytes co-cultured with another liver cell type in serum-free medium. *Biochem Biophys Res Commun* **120**:311–317.

Hewitt NJ, Lechón MJ, Houston JB, Hallifax D, Brown HS, Maurel P, Kenna JG, Gustavsson L, Lohmann C, and Skonberg C, et al. (2007) Primary hepatocytes: current understanding of the regulation of metabolic enzymes and transporter proteins, and pharmaceutical practice for the use of hepatocytes in metabolism, enzyme induction, transporter, clearance, and hepatotoxicity studies. *Drug Metab Rev* **39**: 159–234.

Hoebe KH, Monshouwer M, Witkamp RF, Fink-Gremmels J, and van Miert AS (2000) Cocultures of porcine hepatocytes and Kupffer cells as an improved in vitro model for the study of hepatotoxic compounds. *Vet Q* **22**:21–25.

Hoebe KH, Witkamp RF, Fink-Gremmels J, Van Miert AS, and Monshouwer M (2001) Direct cell-to-cell contact between Kupffer cells and hepatocytes augments endotoxin-induced hepatic injury. *Am J Physiol Gastrointest Liver Physiol* **280**:G720–G728.

Kaji H and Kume T (2005) Regioselective glucuronidation of denopamine: marked species differences and identification of human udp-glucuronosyltransferase isoform. *Drug Metab Dispos* **33**:403–412.

Khetani SR and Bhatia SN (2006) Engineering tissues for in vitro applications. *Curr Opin Biotechnol* **17**:524–531.

Khetani SR and Bhatia SN (2008) Microscale culture of human liver cells for drug development. *Nat Biotechnol* **26**:120–126.

Kostadinova R, Boess F, Applegate D, Suter L, Weiser T, Singer T, Naughton B, and Roth A (2013) A long-term three dimensional liver co-culture system for improved prediction of clinically relevant drug-induced hepatotoxicity. *Toxicol Appl Pharmacol* **268**:1–16.

LeCluyse EL, Witek RP, Andersen ME, and Powers MJ (2012) Organotypic liver culture models: meeting current challenges in toxicity testing. *Crit Rev Toxicol* **42**:501–548.

Levine A, Zagoory-Sharon O, Feldman R, Lewis JG, and Weller A (2007) Measuring cortisol in human psychobiological studies. *Physiol Behav* **90**:43–53.

Lewis JG, Bagley CJ, Elder PA, Bachmann AW, and Torpy DJ (2005) Plasma free cortisol fraction reflects levels of functioning corticosteroid-binding globulin. *Clin Chim Acta* **359**: 189–194.

Maier P and Milosevic N (1999) [Cocultures between primary parenchymal and non-parenchymal liver cells improve the reliability of results from in vitro toxicity testing]. *ALTEX* **16**:87–89.

Messner S, Agarkova I, Moritz W, and Kelm JM (2013) Multi-cell type human liver microtissues for hepatotoxicity testing. *Arch Toxicol* **87**:209–213.

Milosevic N, Schawalder H, and Maier P (1999) Kupffer cell-mediated differential down-regulation of cytochrome P450 metabolism in rat hepatocytes. *Eur J Pharmacol* **368**: 75–87.

Morse JK and Davis JN (1990) Regulation of ischemic hippocampal damage in the gerbil: adrenalectomy alters the rate of CA1 cell disappearance. *Exp Neurol* **110**:86–92.

Obach RS, Baxter JG, Liston TE, Silber BM, Jones BC, MacIntyre F, Rance DJ, and Wastall P (1997) The prediction of human pharmacokinetic parameters from preclinical and in vitro metabolism data. *J Pharmacol Exp Ther* **283**:46–58.

Pang KS and Rowland M (1977a) Hepatic clearance of drugs. I. Theoretical considerations of a "well-stirred" model and a "parallel tube" model. Influence of hepatic blood flow, plasma and blood cell binding, and the hepatocellular enzymatic activity on hepatic drug clearance. *J Pharmacokinet Biopharm* **5**:625–653.

Pang KS and Rowland M (1977b) Hepatic clearance of drugs. II. Experimental evidence for acceptance of the "well-stirred" model over the "parallel tube" model using lidocaine in the perfused rat liver in situ preparation. *J Pharmacokinet Biopharm* **5**:655–680.

Park SY, Seol JW, Lee YJ, Cho JH, Kang HS, Kim IS, Park SH, Kim TH, Yim JH, and Kim M, et al. (2004) IFN-gamma enhances TRAIL-induced apoptosis through IRF-1. *Eur J Biochem* **271**:4222–4228.

Perogamvros I, Aarons L, Miller AG, Trainer PJ, and Ray DW (2011a) Corticosteroid-binding globulin regulates cortisol pharmacokinetics. *Clin Endocrinol (Oxf)* **74**:30–36.

Perogamvros I, Kayahara M, Trainer PJ, and Ray DW (2011b) Serum regulates cortisol bioactivity by corticosteroid-binding globulin-dependent and independent mechanisms, as revealed by combined bioassay and physicochemical assay approaches. *Clin Endocrinol (Oxf)* **75**:31–38.

Perogamvros I, Ray DW, and Trainer PJ (2012) Regulation of cortisol bioavailability—effects on hormone measurement and action. *Nat Rev Endocrinol* **8**:717–727.

Peters T, Jr (1970) Serum albumin. *Adv Clin Chem* **13**:37–111.

Powers MJ, Domansky K, Kaazempur-Mofrad MR, Kalezi A, Capitano A, Upadhyaya A, Kurzawski P, Wack KE, Stolz DB, and Kamm R, et al. (2002a) A microfabricated array bioreactor for perfused 3D liver culture. *Biotechnol Bioeng* **78**:257–269.

Powers MJ, Janigian DM, Wack KE, Baker CS, Beer Stolz D, and Griffith LG (2002b) Functional behavior of primary rat liver cells in a three-dimensional perfused microarray bioreactor. *Tissue Eng* **8**:499–513.

Robin P, Predine J, and Milgrom E (1978) Assay of unbound cortisol in plasma. *J Clin Endocrinol Metab* **46**:277–283.

Roth RA and Ganey PE (2010) Intrinsic versus idiosyncratic drug-induced hepatotoxicity—two villains or one? *J Pharmacol Exp Ther* **332**:692–697.

Roth RA, Luyendyk JP, Maddox JF, and Ganey PE (2003) Inflammation and drug idiosyncrasy—is there a connection? *J Pharmacol Exp Ther* **307**:1–8.

Scheving LA, Buchanan R, Krause MA, Zhang X, Stevenson MC, and Russell WE (2007) Dexamethasone modulates ErbB tyrosine kinase expression and signaling through multiple and redundant mechanisms in cultured rat hepatocytes. *Am J Physiol Gastrointest Liver Physiol* **293**:G552–G559.

Schuetz EG and Guzelian PS (1984) Induction of cytochrome P-450 by glucocorticoids in rat liver. II. Evidence that glucocorticoids regulate induction of cytochrome P-450 by a non-classical receptor mechanism. *J Biol Chem* **259**:2007–2012.

Schuetz EG, Wrighton SA, Barwick JL, and Guzelian PS (1984) Induction of cytochrome P-450 by glucocorticoids in rat liver. I. Evidence that glucocorticoids and pregnenolone 16 alpha-carbonitrile regulate de novo synthesis of a common form of cytochrome P-450 in cultures of adult rat hepatocytes and in the liver in vivo. *J Biol Chem* **259**:1999–2006.

Sivaraman A, Leach JK, Townsend S, Iida T, Hogan BJ, Stolz DB, Fry R, Samson LD, Tannenbaum SR, and Griffith LG (2005) A microscale in vitro physiological model of the liver: predictive screens for drug metabolism and enzyme induction. *Curr Drug Metab* **6**: 569–591.

Sleep D, Cameron J, and Evans LR (2013) Albumin as a versatile platform for drug half-life extension. *Biochim Biophys Acta* **1830**:5526–5534.

Strober W (2001) Trypan blue exclusion test of cell viability. *Curr Protoc Immunol* **3** (Appendix):3B.

Sunman JA, Hawke RL, LeCluyse EL, and Kashuba AD (2004) Kupffer cell-mediated IL-2 suppression of CYP3A activity in human hepatocytes. *Drug Metab Dispos* **32**:359–363.

Tayman C, Rayyan M, and Allegaert K (2011) Neonatal pharmacology: extensive interindividual variability despite limited size. *J Pediatr Pharmacol Ther* **16**:170–184.

Thoma CR, Zimmermann M, Agarkova I, Kelm JM, and Krek W (2014) 3D cell culture systems modeling tumor growth determinants in cancer target discovery. *Adv Drug Deliv Rev* **69-70**: 29–41.

Vivares A, Salle-Lefort S, Arabeyre-Fabre C, Ngo R, Penarier G, Bremond M, Moliner P, Gallas JF, Fabre G, and Klieber S (2015) Morphological behaviour and metabolic capacity of cryopreserved human primary hepatocytes cultivated in a perfused multiwell device. *Xenobiotica* **45**:29–44.

Wang WW, Khetani SR, Krzyzewski S, Duignan DB, and Obach RS (2010) Assessment of a micropatterned hepatocyte coculture system to generate major human excretory and circulating drug metabolites. *Drug Metab Dispos* **38**:1900–1905.

Zinchenko YS, Schrum LW, Clemens M, and Coger RN (2006) Hepatocyte and kupffer cells cocultured on micropatterned surfaces to optimize hepatocyte function. *Tissue Eng* **12**:751–761.

Address Correspondence to: Steven R. Tannenbaum, Department of Biological Engineering, MIT Room 56-731, Massachusetts Institute of Technology, 77 Massachusetts Avenue, Cambridge, MA 02139. E-mail: srt@mit.edu; or John S. Wishnok, Department of Biological Engineering, MIT Room 56-747B, Massachusetts Institute of Technology, 77 Massachusetts Avenue, Cambridge, MA 02139. E-mail: wishnok@mit.edu